International Journal of Thermophysics, Vol. 15, No. 2, 1994

Thermal Diffusivity of POCO AXM-5Q1 Graphite in the Range 1500 to 2500 K Measured by a Laser-Pulse Technique

T. Baba,[1,2] and A. Cezairliyan[1]

Received September 15, 1993

The thermal diffusivity of POCO AXM-5Q1 graphite was measured in the temperature range 1500 to 2500 K utilizing the laser-pulse technique. The uncertainty of the values is estimated to be no more than 3%. The measured values are compared with the results of other investigators.

KEY WORDS: graphite; high temperatures; laser-pulse method; reference material; thermal diffusivity.

1. INTRODUCTION

The laser-pulse method is possibly the most reliable and preferred method for measuring the thermal diffusivity of solid materials at temperatures above 1500 K [1]. Because of this, there is a serious need for reference materials for thermal diffusivity. Although several studies have been undertaken to establish reference materials for thermal diffusivity, as of now no reference material is available that is certified by official national and international organizations.

One of the candidate reference materials for thermal diffusivity at high temperatures up to 2000 K is POCO AXM-5Q1 graphite. Round-robin measurements of the thermal conductivity and thermal diffusivity of POCO AXM-5Q graphite were conducted under the auspices of AFML-AGARD from 1965 to 1972 and the recommended values were given [2]. Later, several leading laboratories participated in a cooperative project under

[1] Metallurgy Division, National Institute of Standards and Technology, Gaithersburg, Maryland 20899, U.S.A..

[2] Guest Scientist from the Thermophysical Metrology Department, National Research Laboratory of Metrology, Tsukuba, Ibaraki 305, Japan.

0195-928X/94/0300-0343$07.00/0

the auspices of CODATA to measure the thermal diffusivity of POCO AXM-5Q1 graphite. However, the resultant quantity of data at high temperatures (above 2000 K) has been limited because there are few laser-pulse apparatuses which are operational at very high temperatures.

The present paper reports the results of accurate measurements of the thermal diffusivity of POCO AXM-5Q1 graphite in the temperature range 1500 to 2500 K performed by the laser-pulse apparatus developed at the U.S. National Institute of Standards and Technology (NIST). Details regarding the construction and operation of the measurement system, the methods of measuring experimental quantities, and other pertinent information such as the formulation for determining thermal diffusivity, error analyses, etc., are given in the preceding paper [3].

2. MEASUREMENTS

2.1. Specimens

A POCO AXM-5Q1 graphite rod (No. 035) was obtained from the Office of Standard Reference Materials (OSRM) at NIST. The rod was 35.6 cm in length and 6.4 mm in diameter. Measurements with a Kelvin bridge yielded a value of 15.92 $\mu\Omega \cdot$ m for the electrical resistivity of the rod. The rod was subsequently machined to a diameter of 6.30 mm to fit the specimen holder.

Six specimens of three different thicknesses, approximately 1.5, 2.0, and 2.5 mm, were cut from the rod. Both the front and the back surfaces of each specimen were polished to optical flatness. The thicknesses at five points were measured for each specimen with a coordinate measuring machine with an uncertainty of 1 μm. The representative thicknesses of the six specimens measured at the center and their flatness are listed in Table I. The average density of the six specimens, calculated from the measured

Table I. Thickness of POCO AXM-5Q1 Graphite Specimens

Specimen No.	Thickness (mm)	Nonuniformity (μm)
1	2.424	10
2	1.945	5
3	1.474	5
4	2.418	10
5	1.955	5
6	1.476	5

weights and dimensions, is 1738 kg · m $^{-3}$. This value is consistent with the density values reported by Hust [4].

2.2. Procedure

A specimen mounted in the tungsten holder was placed inside the experiment chamber. The chamber was evacuated to a pressure less than 1×10^{-3} Pa using a vacuum system consisting of a mechanical pump, a diffusion pump, and a trap cooled by liquid nitrogen. A He–Ne laser beam collimated with the Nd–glass laser beam was used to align the latter to the front surface of the specimen optically. The detector optics and the back surface of the specimen were aligned by using a guide beam introduced from the detector side of the optical system. The detected area is a circle (2 mm in diameter) located at the center of the specimen. Possible movement of the specimen during a series of experiments was monitored by the projection of the He–Ne laser beam on the front surface of the specimen.

A series of experiments was performed on a given day covering the temperature range 1500 to 2500 K in steps of about 100 K. The furnace, and thus the specimen's, temperature was set by adjusting the AC current through the heater element. The temperature of the specimen stabilized within about 20 min after a change in the heater power. Experiments were performed no earlier than 5 min after the steady-state temperature condition was established, provided that the specimen temperature drifted by no more than 0.01 K · s $^{-1}$ below 2200 K or 0.05 K · s $^{-1}$ above 2200 K. Stability of the specimen temperature was noted by monitoring the output of the silicon photodiode detector with a storage oscilloscope.

The experiment was initiated by the discharge of the Nd-glass laser. The digital oscilloscope used to record the data was triggered by the output of the photodiode responding to a small portion of the laser pulse. During an experiment, 4048 data were taken at 100-μs intervals for specimens about 1.5 mm thick or at 200-μs intervals for specimens about 2.0 and 2.5 mm thick.

The steady-state temperature of the specimen was measured with an automatic optical pyrometer immediately before an experiment. The data recorded by the digital oscilloscope were stored on a computer disk. At the end of a series of experiments, the data were transferred to a computer and were processed to calculate the thermal diffusivity values.

2.3. Temperature History Curve and Data Analysis

The solid curve in Fig. 1 shows a typical example of the measured history curve of the transient temperature rise on the back surface of a

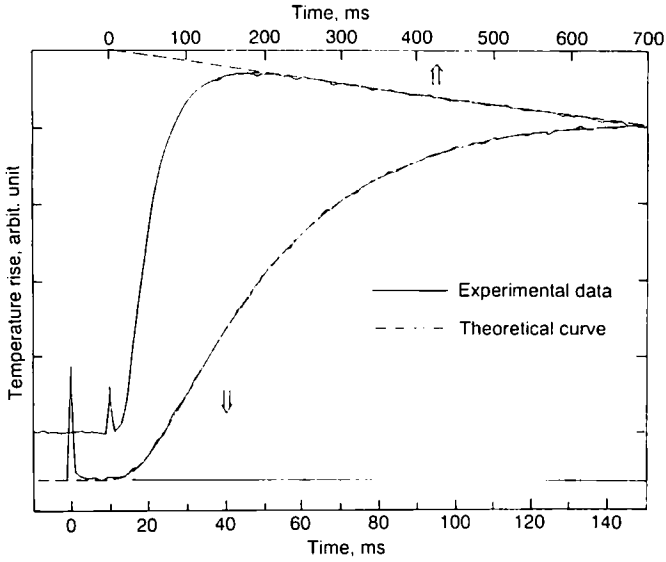

Fig. 1. Typical transient temperature rise curve of thermal diffusivity measurements of POCO AXM-5Q1 graphite using the laser-pulse apparatus. The specimen thickness is 1.945 mm and the specimen temperature is 1696 K. The calculated thermal diffusivity is 0.1137 $cm^2 \cdot s^{-1}$ and the Biot number is 0.05176.

POCO AXM-5Q1 specimen (1.945 mm in thickness at room temperature) at 1696 K. The maximum temperature rise, T_{max}, was 7 K and the peak-to-peak noise level was 0.08 K. This noise is attributed to the electronics, which compensate the steady-state component of the output from the silicon photodiode and amplify the subtracted transient component. The baseline was stable to better than 0.01 $K \cdot s^{-1}$. A small spike at time 0 was induced by the stray light from the Nd–glass laser. Time 0 was set at the center of gravity of the laser-pulse energy distribution on the time scale, which was measured with the same detector system used for radiative detection of transient change of the specimen temperature. After the temperature reached its maximum, it decreased exponentially due to radiative heat loss from the surface of the specimen.

The standard method to determine thermal diffusivity from the measured time–temperature curve has been the "$t_{1/2}$ method" [5]. The half-rise time, $t_{1/2}$, defined by the interval required for the back-surface temperature to reach one-half of the maximum temperature rise, is determined from the experimental curve. The thermal diffusivity is calculated as $\alpha = 1.370l^2/(\pi^2 t_{1/2})$, where l is the thickness of the specimen. The advantage of the $t_{1/2}$ method is its simplicity.

The original $t_{1/2}$ method is valid under the following conditions: (i) the duration of the laser pulse is negligibly short, (ii) the specimen is adiabatic to the environment, (iii) the front surface of the specimen is heated uniformly, (iv) the specimen is homogeneous, and (v) the specimen is opaque.

However, some of the above conditions are not completely satisfied in the actual experiments. Radiative heat loss from the specimen surfaces is unavoidable in high-temperature experiments. It has also been noted [6] that beam profiles from high-energy pulsed lasers are usually not uniform enough for precise thermal diffusivity measurements. Although several modifications of the $t_{1/2}$ method considering the effect of radiative heat loss have been proposed [7–9], they cannot deal effectively with other sources of error, such as the effect of nonuniform heating.

We have introduced a new method of data processing to calculate thermal diffusivity values from the entire transient temperature curve. This "curve-fitting method" is quite different from other methods such as the $t_{1/2}$ method [5] and the recently proposed logarithmic method [10–12], in which the thermal diffusivity value is calculated from only a portion of the time–temperature curve. In this method the experimental data are fitted by Cape and Lehman's theoretical curve [13]. The details of the fitting procedure is described in the preceding paper, describing the apparatus [3]. The curve-fitting method has the following advantages: (i) The analysis can be applied to general boundary conditions including the radiative heat loss condition; (ii) the quality of measurements, especially the effect of nonuniform heating, can be judged by the quality of fitting; and (iii) the fitting algorithm is simple and the calculation can be completed in a short time. Hence, thermal diffusivity values can be calculated with a desktop computer.

Cape and Lehman's theoretical curve was fitted to the experimental solid curve and is displayed by the dashed curve in Fig. 1. Since the experimental data are fitted by the theoretical curve remarkably well, it is very difficult to discriminate the dashed curve from the solid curve. On the scale of this figure they lie on top each other. It was found experimentally that the quality of the fitting depends on the spatial profile of the incident pulsed laser beam. The quality of the fitting is expressed numerically by the residual fitting error, which is the average of the absolute deviation between the curve representing the data and the theoretical curve. When the incident laser beam is spatially uniform, the measured curve is fitted well by the theoretical curve with a small residual fitting error. Temperature rise is normalized by the virtual maximum temperature rise "T_{VM}," which was determined by exponentially extrapolating the radiative decay part of the time–temperature curve back to time 0.

The spatial uniformity of the beam profile of the Nd–glass laser

depends on the following conditions: (i) the alignment of the laser cavity, (ii) the surface conditions of the laser rod and mirrors, (iii) the charging level of the high-voltage capacitors, and (iv) the interval of the laser discharge. We have deduced the effect of the interval of the laser discharge on the spatial beam profile from the quality of the fit between the experimental curve and the theoretical curve. The quality of the fit definitely depended on the interval of the laser discharge. The distribution of the energy absorbed at the front surface of the specimen also depends on the portion of the laser beam incident on the specimen. It was experimentally confirmed that the distribution of the energy absorbed at the front surface of the specimen is unchanged and the residual fitting error stays almost the same as long as the above four conditions are unchanged. We performed a series of experiments keeping these conditions unchanged after obtaining a residual fitting error of less than 2×10^{-3} from a trial experiment at 1800 K. The reproducibility of the thermal diffusivity values at the same temperature was about 1% when the data with the residual fitting error of less than 2×10^{-3} were used.

We performed a total of nine series of experiments using six specimens as listed in Table I. Three of the specimens were used twice and the remaining three were used once. Thus, we could check the reproducibility of the thermal diffusivity values up to 2500 K by comparing the results between the first and the second run for each of three specimens of different thicknesses. We could also check for systematic dependence of thermal diffusivity values on the thickness of the specimen (approximately 1.5, 2.0, and 2.5 mm).

Before a pulse experiment, the steady-state temperature of the specimen was measured with an automatic optical pyrometer through a hole in the side of the specimen holder.

3. RESULTS

The results of thermal diffusivity measurements for the nine runs using the six specimens are represented as a function of temperature in Fig. 2. The list of measured thermal diffusivity values is given in Table AI (Appendix). All the results for the nine runs were merged and fitted by an inverse function of temperature with three variable parameters by means of the least-squares method. The function that was used to represent the final results (standard deviation = 0.95%) for the thermal diffusivity of POCO AXM-5Q1 graphite at temperatures between 1500 and 2500 K is

$$\alpha = 122.4/(T - 156.1) + 0.0342 \qquad (1)$$

where α is in $cm^2 \cdot s^{-1}$ and T is in K. The deviations of the thermal diffusivity values for the nine runs from the fitted function expressed by Eq. (1) are shown in Fig. 3. The deviations are generally less than 2%. Values calculated by Eq. (1) are presented at 100 K intervals in Table II. It should be noted that, in all the computations, the geometrical quantities relating to the specimens are based on their room-temperature (295 K) dimensions; that is, the thermal diffusivity results are presented without any correction for thermal expansion.

There is no systematic difference in the thermal diffusivity results for the first and second runs, which means that POCO AXM-5Q1 graphite is stable at high temperatures at least up to 2500 K. Also, there is no significant dependence of the thermal diffusivity results on the thickness of the specimens, which confirms the following: (i) The total response time of the measurement system to the back-surface temperature rise was fast enough, (ii) the finite pulse-time effect was properly corrected by the center-of-gravity-of-pulse method, and (iii) the effect of radiative heat loss was properly taken into account by the curve-fitting method.

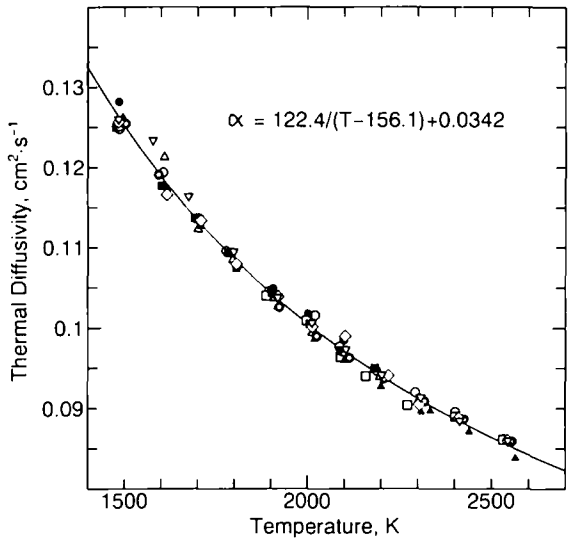

Fig. 2. Thermal diffusivity results for nine runs of six specimens of POCO AXM-5Q1 graphite and the function given by Eq. (1), where ○ is the first run of specimen 1, □ is the first run of specimen 2, △ is the first run of specimen 3, ● is the second run of specimen 1, ■ is the second run of specimen 2, ▲ is the second run of specimen 3, ◯ is the first run of specimen 4, ◇ is the first run of specimen 5, and ▽ is the first run of specimen 6.

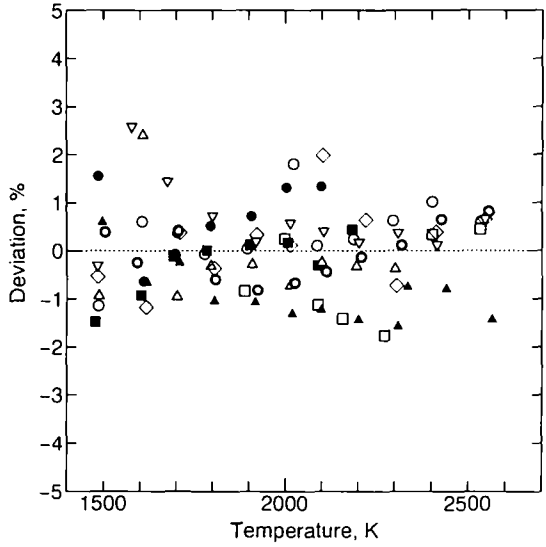

Fig. 3. Deviation of thermal diffusivity results for nine runs of six specimens of POCO AXM-5Q1 graphite from the function given by Eq. (1). Symbols are the same as in Fig. 2.

Table II. Smoothed Thermal Diffusivity α of POCO AXM-5Q1 Graphite According to Eq. (1)

T (K)	α ($cm^2 \cdot s^{-1}$)
1500	0.1253
1600	0.1190
1700	0.1135
1800	0.1087
1900	0.1044
2000	0.1006
2100	0.0972
2200	0.0941
2300	0.0913
2400	0.0887
2500	0.0864

4. ESTIMATE OF ERRORS

Because measurements of thermal diffusivity and of steady-state temperature are independent of each other, their error analyses are given separately. In principle, the thermal diffusivity is obtained from the thickness of the specimen and from some characteristic time in which heat diffuses from the front surface to the back surface of the specimen. Uncertainties associated with the transient temperature curve can be separated into the uncertainties in the determination of the time scale and the uncertainties in the measurement of the transient temperature rise.

The sources of uncertainty mentioned above are related to directly measured quantities. In addition to these, we have to consider other types of uncertainties which are associated with the data analysis and the various corrections for nonideal initial and boundary conditions of heat conduction in real experiments. The major items related to these corrections are the finite pulse time effect, the radiative heat loss, and the nonuniform heating discussed in Section 2.3.

4.1. Uncertainties in Determination of the Steady-State Temperature

Estimation of the uncertainty in the measurement of the steady-state temperature of the specimen is discussed in detail in the preceding paper [3]. The results are summarized in Table III. To assign a corresponding temperature to the measured thermal diffusivity value, the transient maximum temperature rise of the specimen, T_{max}, multiplied by 1.6 is added to the steady temperature of the specimen [5]. The absolute values of T_{max} are estimated from the transient temperature rise curves obtained from the photodiode output, which was calibrated by the pyrometer signal in advance. The values listed in Table III are values of $1.6T_{max}$ when the laser beam with a total power of 42 J was absorbed by POCO AXM-5Q1 graphite 1.5 to 2.5 mm thick. Considering that the area of the specimen is about one-tenth of the total area of the laser beam, these values are consistent with the calculated values by the heat capacity of the specimens [14] assuming that the absorptance of the surface of the specimen is unity.

These $1.6T_{max}$ values, dependent on the specimen thickness, are uniformly added to the steady-state temperature, neglecting the temperature dependence of the specific heat and the fluctuation of the laser-pulse energy. These two effects can be neglected because the ratio of the change of the specific heat of the POCO AXM-5Q1 graphite from 1500 to 2500 K is about 7% and fluctuation of the laser pulse energy is within $\pm 20\%$. Thus, uncertainty associated with the transient temperature rise correction is less

Table III. Sources and Magnitudes of Uncertainties in the Determination of the Steady-State Temperature of the Specimen

Source	Imprecision (K)	Correction (K)	Uncertainty (K)
Standard lamp	0.5	—	2
Pyrometer			
1400–2000 K	1	—	2
1800–2600 K	2	—	4
Quarz window	—	—	2
Temperature difference between cavity and specimen			
1500 K	—	−11	3
2000 K	—	−14	4
2500 K	—	−18	5
Transient temperature rise			
1.5-mm thickness	—	15	5
2.0-mm thickness	—	12	4
2.5-mm thickness	—	9	3
Total maximum uncertainty in steady-state temperature			
1500 K	2	−2 to 4	7
2000 K	2	−5 to 1	8
2500 K	3	−9 to −3	9

than half (30% of 1.6 is 0.48) of T_{max}. Each value of uncertainty for specimens of different thicknesses is listed in Table III.

The total uncertainty in the steady-state temperature obtained from the square root of the total sum of the squares of individual uncertainties is less than 10 K.

4.2. Uncertainties in Thermal Diffusivity Determination

4.2.1. Uncertainties in Measurement of the Specimen Thickness

Uncertainty in the measured thickness of the specimen is less than 0.25% for all the specimens used as listed in Table I. This value corresponds to an uncertainty of 0.5% in the determination of thermal diffusivity.

4.2.2. Uncertainties in Determination of the Time Scale

4.2.2.1. Accuracy of the Time Base of the Total Detection System. This factor is based on the accuracy of the time base of the digital data acquisition system, which is 0.01%.

4.2.2.2. Precision in Determining the Origin of the Time Base. As discussed in our earlier paper [3], the response time of the silicon photodiode and the electronics is less than 10 μs, and the total time resolution of the transient measurement of the specimen's back-surface temperature is determined by the sampling period of the digital oscilloscope. The sampling period is 100 μs for the specimens of 1.5-mm thickness and 200 μs for the specimens of 2.0- and 2.5-mm thickness. The relative delay of the time excursion profile of the Nd–glass laser pulses to the trigger signal for the digital oscilloscope is reproducible within 50 μs.

4.2.2.3. Correction for Finite Pulse Time. The duration of the Nd–glass laser pulse is 550 μs in full width at half maximum. This finite pulse-time effect is corrected by Azumi and Takahashi's center-of-gravity-of-pulse method [15]. Uncertainty in determining the center of gravity of the laser pulse is less than the sampling period of 100 μs.

Compared with the half-rise time $t_{1/2}$, 100 μs over 30 ms is 0.33% in the case of 1.5-mm-thick specimens, 200 μs over 50 ms is 0.4% in the case of 2.0-mm-thick specimens, and 200 μs over 80 ms is 0.25% in the case of 2.5-mm-thick specimens. Thus, uncertainty in thermal diffusivity due to the uncertainty in the time base of the measurements including the finite pulse-time correction is less than 0.5%.

4.2.3. Uncertainties Related to Measurement of the Temperature Signal

Sources and magnitude of uncertainty factors related to the measurement and analysis of the transient temperature signal are listed in Table IV.

4.2.3.1. Uncertainties in Directly Measured Quantities. (a) Drift in the steady-state temperature: Uncertainty of thermal diffusivity due to drift in the steady-state temperature is estimated from the fraction of the drift during 10 times of the half-rise time, $10t_{1/2}$, over the maximum temperature rise T_{max}. The half-rise time $t_{1/2}$ is 30 ms for specimens of 1.5-mm thickness, 50 ms for those of 2.0 mm, and 80 ms for those of 2.5 mm, at 1900 K. Typical values of the drift rate and $1.6T_{max}$ are listed in Tables IV and III, respectively. When the drift rate in the steady-state temperature is 0.01 $K \cdot s^{-1}$, the fraction is $0.01 \times 30 \times 10^{-3} \times 10/9 = 0.04\%$ for a specimen 1.5 mm thick, $0.01 \times 50 \times 10^{-3} \times 10/7 = 0.08\%$ for one 2 mm thick, and $0.01 \times 80 \times 10^{-3} \times 10/5 = 0.16\%$ for one 2.5 mm thick. When the drift rate is 0.05 $K \cdot s^{-1}$, the fraction is 0.2% in the case of a specimen 1.5 mm thick, 0.4% in the case of one 2.0 mm thick, and 0.8% in the case of one 2.5 mm thick. Because the slope of the tangent line at $T(t) = T_{max}/2$ is 1.54 times that of the secant line from that point to the origin, the uncertainty of thermal diffusivity determination is reduced to 1/1.54 of the fraction of drift.

Table IV. Sources and Magnitudes of Uncertainties in the Determination of Transient Temperature Rise and Their Contribution to the Uncertainty in Thermal Diffusivity

Source	Magnitude	Uncertainty in thermal diffusivity (%)
Precision and repruducibility in determining the flash time of the laser pulse (1.5-mm thickness)	50 μs	0.15
Response time of the detector system (1.5-mm thickness)	10 μs	0.03
Sampling period		
1.5-mm thickness	100 μs	0.3
2.0-mm thickness	200 μs	0.4
2.5-mm thickness	200 μs	0.3
Drift in steady-state temperature		
Below 2200 K	0.01 K · s^{-1}	0.1
At 2500 K	0.05 K · s^{-1}	0.5
Signal-to-noise ratio		
At 1500 K	50	0.5
At 2500 K	>1000	<0.03
Nonlinearity in the detector system	1%	0.1
Radiative heat loss correction[a]		
At 1700 K	5%	0.25
At 2200 K	10%	0.5
At 2500 K	18%	0.9
Nonuniform heating effect	8%	1.5[b]

[a] For a specimen 2.5 mm thick.
[b] After screening by the curve-fitting method.

(b) Noise level of the transient temperature signal: Below 1500 K, the radiation detected by the silicon photodiode decreases rapidly as the measurement temperature decreases because of the nonlinearity of Planck's law. For example, the signal-to-noise ratio falls to a value as low as 50 at 1477 K as shown in Fig. 4. The uncertainty in the determination of thermal diffusivity due to the poor signal-to-noise ratio is estimated by shifting the part analyzed by the curve-fitting method. Table V lists the thermal diffusivity values calculated by shifting the analyzed segment of 10-ms duration by a 10-ms step. The standard deviation of the nine values is 0.47%. These data are an example of the lowest signal-to-noise ratio. It

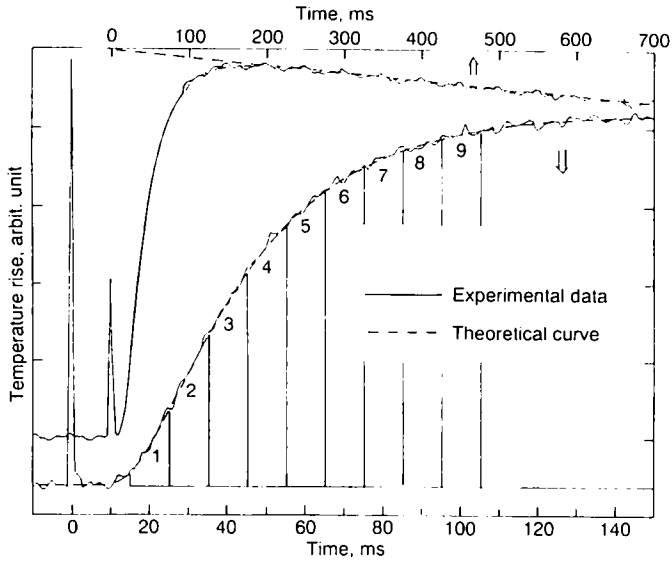

Fig. 4. Example of transient temperature data for the poorest signal-to-noise ratio and segmentally analyzed sections of POCO AXM-5Q1 graphite. The specimen thickness is 1.945 mm and the specimen temperature is 1477 K.

should be noted that the thermal diffusivity values calculated from sections 1, 7, 8, and 9 are more sensitive to the noise than those from other sections. Thus, the uncertainty of the thermal diffusivity due to the noise over the transient temperature signal is expected to be less than 0.1% except in the temperature region close to 1500 K.

Table V. Thermal Diffusivity α Calculated from Different Segments of the Experimental Data

Section No.	Analyzed part (ms)	α ($cm^2 \cdot s^{-1}$)	Deviation (%)
1	15–25	0.1297	0.23
2	25–35	0.1294	0
3	35–45	0.1288	−0.46
4	45–55	0.1295	0.08
5	55–65	0.1295	0.08
6	65–75	0.1298	0.31
7	75–85	0.1305	0.85
8	85–95	0.1282	−0.93
9	95–105	0.1291	−0.23

(c) Nonlinearity of the detector system: Nonlinearity of the total detector system, which is due mainly to Planck's law as described in the preceding paper [3], is estimated to be less than 1% for the transient maximum temperature rise of 10 K. The uncertainty of the thermal diffusivity determination due to this effect is less than 0.1%.

4.2.4. Uncertainties Associated with Data Analysis

4.2.4.1. Finite Pulse-Time Correction. The uncertainty in the determination of the center of gravity of the laser pulse is better than 100 μs as stated in the previous section. The associated uncertainty in thermal diffusivity is less than 0.5% when the FWHM of the laser pulse is 550 μs and the half-rise time $t_{1/2}$ is 20 ms.

4.2.4.2. Heat Loss Correction. The thermal diffusivity values are determined by the first type of program in the curve-fitting method, which considers radiative heat loss only in the axial direction. It was estimated in the preceding paper [3] that the uncertainty from the anisotropy of radiation heat loss is less than 5% of the magnitude of the radiative heat loss correction. The validity of the curve-fitting method for radiative heat loss correction is supported by the small scattering in the thermal diffusivity values at high temperatures independent of the specimen thickness; the standard deviation is less than 1% up to 2500 K for AXM-5Q1 specimens having thicknesses of 1.5, 2.0, and 2.5 mm.

4.2.4.3. Nonuniform Heating. As described in the preceding paper [3], the scatter in the apparent thermal diffusivity values may be as large as 8% when arbitrary parts of the irregular laser beam are randomly chosen to impinge on the surface of the specimen. The profile of the laser beam is reproducible from pulse to pulse under the same alignment of the laser, the same charging voltage, and the same interval in consecutive discharging of the laser. This reproducibility is demonstrated by the reproduction of the same pattern of the deviation between the theoretical and the experimental curves.

The most uniform heating condition was determined by shifting the position of the laser beam incident onto the specimen, changing the interval of discharging the laser pulse, and if necessary, adjusting the alignment of the laser cavity until a close fit between the experimental and the theoretical curves is obtained with an averaged residual fitting error of less than 0.01%. After these conditions are established, a series of experiments in the range 1500–2500 K is made, where the uncertainty in the thermal diffusivity due to nonuniform heating error is not more than 1.5%. It should be noted that the nonuniform heating error is basically independent

of the measurement temperature since it is a function of the specimen thickness-to-diameter ratio and of the profile of the laser beam, which is reproducible during a series of experiments.

4.3. Summary of Error Analysis

Based on the detailed analysis of uncertainties given in the previous sections, the imprecision and uncertainty of the thermal diffusivity determination are summarized in Table VI. The uncertainty of the steady-state temperature is 7 K at 1500 K and 9 K at 2500 K. The uncertainty of the thickness of the specimen is less than 0.25%. This value contributes an uncertainty of 0.5% to the thermal diffusivity since the thermal diffusivity is related to the square of the specimen thickness.

The square root of the sum of the squares of uncertainties due to precision and reproducibility in determining the flash time of the laser pulse, response time of the detector system, and sampling period is compiled as uncertainty in determination of the time scale. The square root of the sum of the squares of uncertainties due to drift in the steady-state temperature, signal-to-noise ratio, and nonlinearity in the detector system is compiled as uncertainty in measurement of the temperature signal. The square root of the sum of the squares of uncertainties from radiative heat loss correction and nonuniform heating effect is compiled as uncertainty in data analysis and corrections. The uncertainly in thermal diffusivity, obtained from the square root of the sum of the squares of these four individual uncertainties in Table VI, is estimated to be not more than 3%.

Uncertainty in the difference between the specimen temperature and the radiance temperature inside of the specimen holder is the major contributor to the total uncertainty in the measurement of the steady-state

Table VI. Summary of the Error Analysis

Quantity	Imprecision		Uncertainty	
	1500 K	2500 K	1500 K	2500 K
Steady-state temperature (K)	2	3	7	9
Thickness of the specimen				
In length (%)	0.05	0.05	0.25	0.25
In thermal diffusivity (%)	0.1	0.1	0.5	0.5
Determination of time scale (%)	0.4	0.4	0.5	0.5
Measurement of temperature signal (%)	0.5	0.5	0.6	0.6
Data analysis and corrections (%)	1.5	1.5	1.6	1.8
Thermal diffusivity (%)	2	2	3	3

temperature. Nonuniform heating effect is the major contributor to the uncertainty in thermal diffusivity even after the data under the irradiation of less irregular beams are selected by the data analysis. In the case of POCO AXM-5Q1 graphite, an uncertainty of 10 K in the steady-state temperature at 1500 K corresponds to an uncertainty of 0.5% in thermal diffusivity. Thus, it is necessary to reduce the uncertainty in the steady-state temperature as well as the uncertainty in the thermal diffusivity itself to reduce the total uncertainty of thermal diffusivity data at high temperatures.

5. DISCUSSION

A comparison of our results for thermal diffusivity with other literature data on graphite of the same grade is presented in Fig. 5 [16–19]. The specimen material for each investigation was obtained from the same lot of POCO AXM-5Q1 graphite (available at OSRM at NIST [4]). The literature data of the thermal diffusivity were obtained by the laser-pulse method with one exception: Brandt and Neuer [16] used a xenon-lamp modulated-beam method. The results obtained by Taylor and Groot [19] and the results for the first specimen reported by Brandt and Neuer [16] are in good agreement with those of the present work; the other

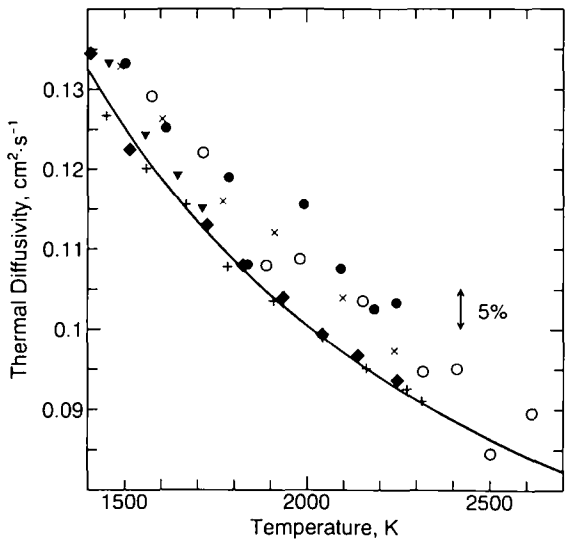

Fig. 5. Comparison of the present values for the thermal diffusivity of POCO AXM-5Q1 graphite with the literature values; ○ and ● are from Taylor [18], + and × are from Brandt and Neuer [16], ▼ is from Maglić et al. [17], and ◆ is from Taylor and Groot [19].

Table VII. Characteristics of POCO AXM-5Q1 Graphite Specimens Measured by Other Investigators

Investigator(s)	Symbol	Density ($kg \cdot m^{-3}$)	Electrical resistivity ($\mu\Omega \cdot m$)
	In Fig. 5		
Taylor [18]	○	1751	13.12
	●	1707	15.29
Brandt and Neuer [16]	+	1733	14.31
	×	1723	14.88
Maglić et al. [17]	▼	1755	14.59
Taylor and Groot [19]	◆	1694	14.70
	In Fig. 6		
Hust [4] (NIST standard value)	------	1730	14.50
	In Figs. 5 & 6		
Present work	——	1738	15.92

results give values somewhat higher than the present results. The discrepancies amount to about 10%. These discrepancies cannot be explained by the differences in the density and in the electrical resistivity of the various specimens, which are tabulated in Table VII. For example, the two curves of Brandt and Neuer are biased in the opposite direction from that expected from considerations of the density and the electrical resistivity differences. Two diffusivity curves of Taylor [18] are close to each other in spite of the considerable difference in the corresponding electrical resistivity values.

A comparison of our results with the recommended values for POCO AXM-5Q1 and POCO AXM-5Q[3] graphite is presented in Fig. 6. The present results are slightly higher than the long-dashed curve, which is the representative curve given by AGARD for POCO AXM-5Q graphite in Ref. 2. The deviation is less than 2%. The thermal diffusivity curve of the present work crosses the short-dashed curve, which represents the thermal diffusivity values recommended by Hust without density and electrical resistivity correction [4]. The difference between the two curves is less than 5%.

Hust analyzed the correlation between thermal conductivity and density and electrical resistivity from the measurements of these quantities for 13

[3] AXM-5Q is a POCO grade of slightly lower purity than AXM-5Q1.

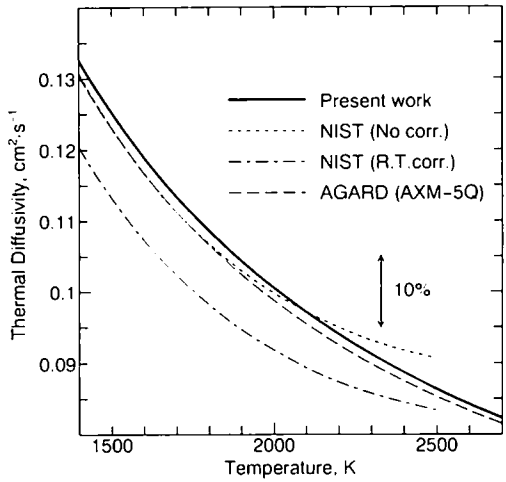

Fig. 6. Comparison of the present values for the thermal diffusivity of POCO AXM-5Q1 graphite with the values recommended in the literature.

POCO AXM-5Q1 graphite specimens at room temperature. He proposed the following equation for the thermal conductivity of POCO AXM-5Q1 graphite λ ($W \cdot m^{-1} \cdot K^{-1}$) as a function of the density d_0 ($kg \cdot m^{-3}$) and the electrical resistivity ρ_0 ($\mu\Omega \cdot m$), both at room temperature:

$$\lambda = [(-18.51 + 0.01908 d_0)/\rho_0]\,\lambda_s \tag{2}$$

where λ_s is the thermal conductivity without the room temperature correction when $d_0 = 1730\ kg \cdot m^{-3}$ and $\rho_0 = 14.5\ \mu\Omega \cdot m$ [4]. The short-dashed curve in Fig. 6 corresponds to the temperature dependence of α corresponding to λ_s without room-temperature correction. The average density and electrical resistivity of the graphite rod designated 035 are $1738\ kg \cdot m^{-3}$ and $15.92\ \mu\Omega \cdot m$, respectively. Substituting these values in Eq. (2) we obtain $\lambda = 0.920\ \lambda_s$. It can be assumed that thermal diffusivity α is proportional to λ because heat capacity is insensitive to density and electrical resistivity. The dash-dotted curve corresponds to the temperature dependence of α calculated from this λ with room-temperature correction. The curve of the present work is much closer to the uncorrected curve than the corrected curve. According to the NIST data for rod 035 of 6.3-mm diameter [4], the resistivity of the notched end is $16.37\ \mu\Omega \cdot m$ and that of the other end is $15.78\ \mu\Omega \cdot m$, which results in a 3.7% difference. The thermal diffusivities of specimens cut from both ends of rod 035 were measured and there was no significant difference (less than 1%) between them. These

results mean that the room-temperature correction by Eq. (2) is not effective for high-temperature measurements such as those in the present work.

At present, there are not enough data at high temperatures to correlate thermal diffusivity with density and electrical resistivity successfully. It is difficult to say whether differences among the literature results on the thermal diffusivity of POCO AXM-5Q1 graphite at high temperatures are related to systematic measurement errors or to real differences of thermal diffusivity due to the variabilities of POCO AXM-5Q1 graphite. One possible approach is to measure the thermal diffusivity of many specimens of well-characterized POCO AXM-5Q1 graphite systematically at high temperatures to reach a clear conclusion about the correlation. Another approach is to search for other materials with less variability in thermal diffusivity than POCO AXM-5Q1 for a standard reference material for thermal diffusivity and thermal conductivity.

APPENDIX

Table AI. Experimental Results for the Thermal Diffusivity α of POCO AXM-5Q1 Graphite

T (K)	α ($cm^2 \cdot s^{-1}$)	$\Delta\alpha$ (%)[a]
	Specimen 1, Run 1	
1486	0.1248	−1.14
1605	0.1194	0.61
1696	0.1136	−0.08
1778	0.1096	−0.06
1896	0.1046	0.05
2022	0.1016	1.81
2087	0.0977	0.11
2187	0.0947	0.24
2295	0.0920	0.63
2402	0.0896	1.02
2534	0.0862	0.61
	Specimen 1, Run 2	
1486	0.1282	1.56
1609	0.1177	−0.63
1702	0.1138	0.37
1794	0.1095	0.52
1906	0.1049	0.72
2003	0.1018	1.32
2099	0.0985	1.34

[a] The percentage deviation of the individual results from the smooth function defined by Eq. (1).

Table AI. *(Continued)*

T (K)	α ($cm^2 \cdot s^{-1}$)	$\Delta\alpha$ (%)[a]
	Specimen 2, Run 1	
1888	0.1040	−0.83
1998	0.1009	0.25
2090	0.0964	−1.12
2158	0.0940	−1.41
2273	0.0904	−1.76
2402	0.0890	0.34
2532	0.0861	0.45
	Specimen 2, Run 2	
1477	0.1250	−1.47
1603	0.1177	−0.92
1693	0.1137	−0.12
1784	0.1094	0.01
1903	0.1044	0.13
2007	0.1005	0.17
2090	0.0972	−0.30
2183	0.0950	0.44
	Specimen 3, Run 1	
1487	0.1250	−0.93
1609	0.1213	2.41
1702	0.1123	−0.95
1796	0.1085	−0.31
1910	0.1037	−0.28
2013	0.0994	−0.72
2101	0.0969	−0.24
2196	0.0939	−0.32
2302	0.0909	−0.37
	Specimen 3, Run 2	
1496	0.1263	0.60
1619	0.1171	−0.65
1710	0.1127	−0.24
1805	0.1073	−1.04
1917	0.1026	−1.07
2019	0.0986	−1.31
2099	0.0960	−1.23
2201	0.0927	−1.44
2310	0.0896	−1.57
2335	0.0897	−0.75
2440	0.0871	−0.79
2565	0.0838	−1.43

Table AI. *(Continued)*

T (K)	α ($cm^2 \cdot s^{-1}$)	$\Delta\alpha$ (%)[a]
	Specimen 4, Run 1	
1504	0.1255	0.39
1593	0.1191	−0.24
1705	0.1137	0.42
1807	0.1077	−0.59
1924	0.1026	−0.81
2026	0.0990	−0.66
2114	0.0963	−0.43
2209	0.0937	−0.13
2319	0.0909	0.12
2426	0.0887	0.65
2556	0.0859	0.82
	Specimen 5, Run 1	
1484	0.1257	−0.53
1617	0.1166	−1.17
1710	0.1134	0.38
1806	0.1080	−0.36
1921	0.1039	0.34
2014	0.1002	0.12
2103	0.0990	1.99
2220	0.0941	0.64
2305	0.0905	−0.72
2412	0.0888	0.39
2545	0.0860	0.66
	Specimen 6, Run 1	
1484	0.1260	−0.30
1578	0.1234	2.59
1676	0.1164	1.45
1799	0.1095	0.73
1920	0.1038	0.20
2013	0.1007	0.58
2105	0.0974	0.41
2202	0.0942	0.18
2309	0.0914	0.38
2415	0.0885	0.13
2545	0.0860	0.66

ACKNOWLEDGMENTS

One of the authors (T.B.) acknowledges the support of his organization (NRLM) and NIST during his stay as a guest scientist at NIST.

REFERENCES

1. F. Righini and A. Cezairliyan, *High Temp.-High Press.* **5**:481 (1973).
2. E. Fitzer, AGARD Report 606 (AGARD, NATO, France, 1972), p. 35.
3. A. Cezairliyan, T. Baba, and R. Taylor, *Int. J. Thermophys.* **15**:317 (1994).
4. J. G. Hust, A Fine-Grained, Isotropic Graphite for Use as NBS Thermophysical Property RM's from 5 to 2500 K, Special Publ. 260-89 (Natl. Bur. Stand., U.S., 1984).
5. W. J. Parker, R. J. Jenkins, C. P. Butler, and G. L. Abbott, *J. Appl. Phys.* **32**:1679 (1961).
6. T. Baba, M. Kobayashi, A. Ono, J. H. Hong, and M. M. Suliyanti, *Thermochim. Acta* **218**:329 (1993).
7. R. D. Cowan, *J. Appl. Phys.* **14**:926 (1963).
8. L. M. Clark III and R. E. Taylor, *J. Appl. Phys.* **46**:714 (1975).
9. Y. Takahashi, T. Azumi, and M. Sugano, *Netsu Sokutei* **8**:62 (1981) (in Japanese).
10. Y. Tada, M. Harada, M. Tanigaki, and W. Eguchi, *Rev. Sci. Instrum.* **49**:1305 (1978).
11. H. M. James, *J. Phys.* **51**:4666 (1980).
12. Y. Takahashi, K. Yamamoto, and T. Ohsato, *Netsu Sokutei* **15**:103 (1988) (in Japanese).
13. J. A. Cape and G. W. Lehman, *J. Appl. Phys.* **34**:1909 (1963).
14. A. Cezairliyan and A. P. Miiller, *Int. J. Thermophys.* **6**:285 (1985).
15. T. Azumi and Y. Takahashi, *Rev. Sci. Instrum.* **52**:1411 (1981).
16. R. Brandt and G. Neuer, in *Proceedings of the 17th International Thermal Conductivity Conference*, J. G. Hust, ed. (Plenum, New York, 1983), p. 117.
17. K. Maglić, N. Perovic, and Z. Zivotic, in *Proceedings of the 17th International Thermal Conductivity Conference*, J. G. Hust, ed. (Plenum, New York, 1983), p. 163.
18. R. Taylor, in *Proceedings of the 17th International Thermal Conductivity Conference*, J. G. Hust, ed. (Plenum, New York, 1983), p. 753.
19. R. E. Taylor and H. Groot, *High Temp.-High Press.* **12**:147 (1980).